Published in final edited form as:
Dev Biol. 2013 January 1; 373(1): 72–82. doi:10.1016/j.ydbio.2012.10.010.

Generalized disruption of inherited genomic imprints leads to wide-ranging placental defects and dysregulated fetal growth

K. P. Himes[a], **E. Koppes**[b], and **J. Richard Chaillet**[b]

[a]Magee-Womens Research Institute, Department of Obstetrics, Gynecology and Reproductive Sciences, University of Pittsburgh School of Medicine, 204 Craft Avenue Pittsburgh, PA 15213 USA

[b]Magee-Womens Research Institute, Department of Microbiology and Molecular Genetics, University of Pittsburgh School of Medicine, 204 Craft Avenue Pittsburgh, PA 15213 USA

Abstract

Monoallelic expression of imprinted genes, including ones solely expressed in the placenta, is essential for normal placental development and fetal growth. To better understand the role of placental imprinting in placental development and fetal growth, we examined conceptuses developing in the absence of maternally derived DNA (cytosine-5-)- methyltransferase 1o (DNMT1o). Absence of DNMT1o results in the partial loss of methylation at imprinted differentially methylated domain (DMD) sequences in the embryo and the placenta. Mid-gestation E9.5 DNMT1o-deficient placentas exhibited structural abnormalities of all tissue layers. At E17.5, all examined placentas had aberrant placental morphology, most notably in the spongiotrophoblast and labyrinth layers. Abnormalities included an expanded volume fraction of spongiotrophoblast tissue with extension of the spongiotrophoblast layer into the labyrinth. Many mutant placentas also demonstrated migration abnormalities of glycogen cells. Additionally, the volume fraction of the labyrinth was reduced, as was the surface area for maternal fetal gas exchange. Despite these placental morphologic abnormalities, approximately one-half of DNMT1o-deficient fetuses survived to late gestation (E17.5). Furthermore, DNMT1o- deficient placentas supported a broad range of fetal growth. The ability of some DNMT1o-deficient and morphologically abnormal placentas to support fetal growth in excess of wild type demonstrates the importance of differential methylation of DMDs and proper imprinting of discrete gene clusters to placental morphogenesis and fetal growth.

Keywords

Imprinting; Placenta; Fetal growth; DNMT1; Methylation

INTRODUCTION

Genomic imprinting is a highly conserved epigenetic process that distinguishes parental alleles of a small number of genes such that only one parental allele is transcriptionally active. For the majority of imprinted genes, this difference is absolute; one allele is

Corresponding author: J. Richard Chaillet, chailletjr@mwri.magee.edu, phone: (412) 641-8166.

expressed and the opposite allele is silent (Bartolomei and Tilghman 1997). With few exceptions, the approximately 100 known mouse imprinted genes are organized into 16 clusters (http://www.mousebook.org/catalog.php?catalog=imprinting.) harboring a variable number of imprinted genes. Importantly, the imprinted, monoallelic expression of genes in the same cluster is determined by a small contiguous set of sequences called the imprint control region (ICR) (Reinhart et al. 2002). In general, deletion of ICR sequences leads to complete (biallelic) transcriptional silencing or to biallelic expression, depending on the cluster and the particular gene in the cluster. These findings are consistent with the notion that imprinted gene expression is a complex regulatory phenomenon involving many *cis*- and *trans*-acting factors, but mediated primarily through ICRs (Reinhart and Chaillet 2005).

The function of ICR sequences in regulating the imprinted expression of genes appears to be largely determined by differentially methylated domains (DMDs) within the ICR sequence. DMDs originate during gametogenesis through the action of DNA (cytosine-5-)-methyltransferase 3 alpha (Bourc'his et al., 2001; Hata et al., 2002; Kaneda et al., 2004). After fertilization, DMD methylation is maintained in all cells of the conceptus by different isoforms of the DNMT1 cytosine-5 methyltransferase (Cirio et al., 2008a; Hirasawa et al., 2008).

Proper inheritance of methylation imprints is essential for normal development. Insight into the mechanism of this epigenetic inheritance during preimplantation has come from examining the expression of isoforms of DNMT1. The enzyme DNMT1o exhibits a unique, stage-specific role in the inheritance of DMD methylation during preimplantation. DNMT1o is synthesized in the maternal oocyte and maintains DMD methylation in the 8-cell embryo (Cirio et al., 2008b; Doherty et al., 2002; Howell et al., 2001). In contrast the longer somatic DNMT1s form maintains methylation at other preimplantation cleavage stages (Cirio et al., 2008a; Hirasawa et al., 2008). Post-implantation embryos derived from DNMT1o-deficient oocytes have lost methylation on ~50% of the normally methylated alleles of their DMDs. Loss of DNMT1o results in generation of epigenetic mosaic embryos (Cirio et al., 2008b; Howell et al., 2001; Toppings et al., 2008). These are produced by the combined effects of a loss of DNMT1o maintenance methyltransferase activity followed by the normal process of random chromosome segregation. The loss of methylation leads to altered expression of imprinted genes, manifest as biallelic expression of some genes or loss of expression of most genes. Methylation of non-imprinted DNA is unchanged.

Imprinted genes are highly and in some cases uniquely expressed in the placenta. Of the 16 imprinted gene clusters, seven (*Peg10, H19/Igf2, Mest, Kcnq1, Grb10, Dlk1/Meg3*, and *Igf2r*) are of particular interest. Not only do these clusters contain genes that are highly expressed in the placenta, but mutations in these genes have been associated with placental maldevelopment and/or dysfunction (Frost and Moore 2010). For example, ablation of the maternally expressed allele of *Ascl2* results in fetal death on embryonic day 10.5 (E10.5), with poorly developed labyrinthine vasculature, reduced population of spongiotrophoblasts, and an excess of trophoblast giant cells (Guillemot et al., 1995). Deletion of *Peg10* results in a similar placental phenotype (Ono et al., 2006).

While much has been learned about the role of imprinted genes in placental development from targeted inactivating or over-expressing individual imprinted genes, a comprehensive study of the role of imprinting in placental function should include removal of the inherited DNA methylation at DMD sequences. This can be conferred by DNMT1o deficiency. The loss of DNMT1o in embryos from homozygous $Dnmt1^{\Delta 1o/\Delta 1o}$ female mice provides an opportunity to analyze the functions of multiple imprinted genes by stochastic elimination of DMD methylation at many sites. Here we tested the hypothesis that DNMT1o deficiency adversely affects placental development and function.

MATERIALS AND METHODS

Animals

The mutant *Dnmt1*$^{\Delta 1o}$ allele was maintained in the wild type (wt) 129/SvTac strain background. Embryos derived from wild-type and homozygous *Dnmt1*$^{\Delta 1o/\Delta 1o}$ dams mated with 129/SvTac males were compared. For studies of parent-specific methylation of differentially methylated domains (DMDs), *Dnmt1*$^{\Delta 1o/\Delta 1o}$ or wt 129/Sv/Tac female mice were crossed to inbred CAST/Ei male mice. *Dnmt1*$^{\Delta 1o}$ mice were genotyped using a PCR assay as previously described (Howell et al., 2001). Primers are included in Supplemental Table 2. All experiments were performed in compliance with guidelines established by the Institutional Animal Care and Use Committee of the University of Pittsburgh.

Placenta dissection and extraction

Copulation was determined by the presence of a vaginal plug and embryonic day zero (E0) was assumed to be midnight. Conceptuses were collected from the uteri of female mice at E9.5, E12.5, E15.5 or E17.5. Placentas for DNA and RNA extraction were dissected from embryos, decidua and yolk sac tissue and kept individually in RNALater (Sigma). Placentas for histologic and morphometric analyses were dissected from embryo and yolk sac but decidua was preserved.

Determinations of DMD methylation

Genomic DNA was extracted from E9.5 and 17.5 placentas using AllPrep DNA/RNA Micro Kit and from one half of sagittal sections of E15.5 and E17.5 using AllPrep DNA/RNA Mini Kit(Qiagen). Genomic DNA methylation patterns of DMDs in F1 hybrid mice obtained from crosses between 129/Sv/Tac female mice and CAST/Ei male mice were determined using the method of bisulfite genomic sequencing (Lucifero et al., 2002). Five DNMT1o-deficient E9.5 placentas and six DNMT1o-deficient E17.5 placentas were analyzed. Maternal and paternal alleles were distinguished by single nucleotide polymorphisms in the different DMDs. Primers are included in Supplemental Table 2. For more widespread quantitative methylation analysis the EpiTYPER application (Sequenom) was used as previously described (Ehrich et al., 2005). DNA methylation standards (0, 50, and 100%) were used to correct for bias. Primers for the EpiTYPER experiments are included in Supplemental Table 2.

Standard histology and stereology

Placentas were collected, bisected in the midline and half of placenta fixed overnight at 4°C in 4% paraformaldehyde (PFA) in PBS. Specimens were then dehydrated and embedded in paraffin. Sections (5 μm) were stained with either hematoxylin and eosin or periodic acid-Schiff (PAS) stain. Volume fraction of spongiotrophoblast and labyrinth was determined by counting points that fall in the relevant placental layer compared to total placental reference space. Data is presented as percent spongiotrophoblast or labyrinth of total. Four wild type (two litters) and twelve DNMT1o-deficient placentas from five litters were evaluated.

RNA in situ hybridization (ISH)

E9.5 and E17.5 placentas were dissected in PBS and fixed in fresh 4% PFA. PFA-fixed samples were immersed in 10%, then 20% sucrose in PBS, followed by OCT embedding. We used digoxigenin-labeled cRNA probes, synthesized using digoxigenin RNA labeling kit (Roche, Basel, Switzerland). Cryosections (10 μm) of the OCT-embedded placentas were used for ISH as previously described (Barak et al., 1999).

Immunohistochemistry

Sections (5 μm) were obtained after fixing placentas in 4% PFA overnight, dehydration and paraffin embedding. Immunohistochemistry was performed using the Vectastain Elite ABC kit (Vector laboratories) and DAB substrate per manufacturer recommendations (Vector Labs). To identify fetal endothelium, a 1:200 dilution of rabbit polyclonal anti-CD31 antibody (Abcam-ab28364) was used. Hematoxylin and acid alcohol were used for counter stain. The ratio of vasculature surface area to labyrinthine volume was determined using a cycloid arc grid as previously described (Baddeley et al., 1986; Coan et al., 2004). A cycloid arc grid was overlaid on highmagnification images of CD31 stained sagittal placental sections from wt or DNMT1odeficient placentas. Cycloid line intersections with vascular walls were counted to determine vasculature surface area and points within the reference space counted to determine volume. Measurements were performed on systematic random samples of 24 images per placenta using every fifth section from each placenta. Five wt and 10 DNMT1o-deficient placentas were analyzed. The data are presented as maternal and fetal surface area, and expressed as vasculature surface area per volume of labyrinth (cm^2/cm^3).

Quantitative measurements of imprinted gene transcripts

RNA was extracted using either the AllPrep DNA/RNA Micro or Mini Kit (Qiagen). Contaminating DNA was removed by DNAse treatment according to manufacturer's instruction. Complementary DNA was prepared from 1 μg RNA using the high capacity cDNA reverse transcription kit (Applied Biosystems). RT-qPCR was performed in triplicate using SYBR Green PCR Master Mix (Applied Biosystems) in total reaction volume of 10μl on the 7900HT Fast Real-Time PCR System machine. Primer pairs are listed in Supplementary Table 2. Primer sequences were obtained from Primer Bank or designed using Primer Express. Dissociation curves were run on all reactions to ensure amplification of a single product. A control without RT (- RT) was run for each sample and a control without template (- template) was run for each primer set. Samples were analyzed using the ΔΔCt method. Five wild type placentas were analyzed at each gestational age.

Microarray gene expression studies

RNA was extracted as described above. Illumina Mouse WG-6- v2.0 Expression BeadChips were used for whole genome expression profiling. After normalization mean expression values were determined and compared by t test. Adjusted p values were then calculated to correct for multiple comparisons. Significant genes were defined as those with an adjusted p value < 0.05. Fold changes were calculated and the overlapping and non-overlapping genes between the two placental phenotypes determined. Data were then analyzed through the use of Ingenuity Pathway Analysis (IPA). IPA Functional Analysis identified the biological functions and networks that were most significant among our list of genes. Right-tailed Fisher's exact test was used to calculate a p-value.

Statistical Analysis

Kruskal Wallis was used for nonparametric univariate analysis of continuous variables. Normality was assessed by sktest. Multivariable linear regression was used to assess the independent association between E/P ratio and imprinted gene expression. Gender and other imprinted gene expression were considered as a potential confounder. Given a non-parametric distribution of DMD methylation data Spearman's rank sum was used to determine correlation between placentas. All analyses were done with Stata version 10 (StataCorp).

RESULTS

Epigenetic mosaicism in DNMT1o-deficient placentas

We previously reported a significant loss of methylation from normally methylated parental alleles in both the *H19/Igf2* and *Snurf/Snrpn* DMDs of E9.5 DNMT1o-deficient placentas (Cirio et al. 2008). We extended these findings to additional DMDs and examined DMD methylation in late gestation. As shown in representative placentas in Figure 1, strict parent-specific DMD methylation was observed for all DMDs in a wt E9.5 placenta. In contrast, significant deviations from parent-specific methylation were observed in DMDs of all DNMT1o-deficient placentas (M1–M3). For example, nearly complete loss of *Mest* DMD methylation was observed in all mutant placentas. We also observed placenta-to-placenta variation in the extent of methylation loss at individual DMDs. For example, whereas M1 showed a pattern of strict parent-specific methylation for *Snurf/Snrpn* DMD, M2 showed a near complete loss. In any individual placenta, there was no correlation among the four different DMDs for the extent of methylation loss. For example, M1 showed nearly complete loss of DMD methylation on *H19/Igf2* DMD and *Mest* DMD, yet normal methylation on *Snurf/Snrpn* DMD, whereas M2 showed nearly complete loss of DMD methylation on *Mest, Snurf/Snrpn*, and *Kcnq1* DMD, yet near normal methylation on *H19/Igf2* DMD. Finally, there was no evidence in wt or DNMT1o-deficient placentas of methylation on the normally unmethylated parental allele. We conclude that DNMT1o-deficient placentas are developing during the first half of gestation as cellular mosaics with variable loss of DMD methylation across all DMDs examined.

At E17.5, the type and extent of DMD methylation changes were distinct from those obtained from E9.5 DNMT1o-deficient placentas. For the *Snurf/Snrpn* and *Mest* DMDs, we observed significant loss of DMD methylation in single placentas, with no evidence of acquisition of methylation on the normally unmethylated parental DMD allele. For *H19/Igf2* and *Kcnq1* DMDs, while the normally unmethylated parental allele remained unmethylated in all DNMT1o-deficient placentas, of the six placentas we analyzed methylation of the normally methylated parental allele was not significantly altered. This finding is notably different from *H19/Igf2* and *Kcnq1* DMD methylation in E9.5 DNMT1o-deficient placentas. Finally, as was true at E9.5, there was no evidence in wt or DNMT1o-deficient placentas of methylation on the normally unmethylated parental allele. We conclude from these allele-specific DMD methylation studies that while DMD epigenetic mosaicism is found in late gestational DNMT1o-deficient placentas, the precise makeup of mosaics evolves during the second half of gestation such that it is uncommon to recover certain patterns of DMD methylation.

Temporal progression of imprinted-gene expression in DNMT1o-deficient placentas

To further understand the changes across gestation in DNMT1o-deficient placentas, we used quantitative RT- PCR (RT-qPCR) to determine the expression of a large set of imprinted genes, spanning seven imprinted clusters at E9.5, E12.5, E15.5 and E17.5 (Figure 3). In E9.5 DNMT1o-deficient placentas, we found that average changes in imprinted-gene expression compared to wt levels were consistent with predictions due to changes in DMD methylation. For example, mean *H19* gene expression approximately doubled while mean *Igf2* gene expression approximately halved, as expected for a 50% loss of *H19/Igf2* DMD methylation (Cirio et al. 2008; Howell et al. 2001). Interestingly, the profile of imprinted gene expression at E12.5 resembles the expression pattern seen at E9.5 suggesting that at least until E12.5, imprinted genes are expressed in a manner consistent with their predicted DMD methylation. In contrast, the profiles of imprinted-gene expression at E15.5 and E17.5 changed dramatically (Figure 3). For example, at E17.5 the mean *H19* and *Igf2* expression levels in DNMT1o-deficient placentas were similar to wt levels. Additionally, at both E15.5

and 17.5 genes within the *Dlk1* and *Kcnq1* clusters were increased, a finding contrary to that predicted based on loss of methylation at the DMD. Moreover, we observed a broad spectrum of imprinted-gene expression profiles among individual E17.5 DNMT1o-deficient placentas (Supplemental Table 1).

Highly variable structures of DNMT1o-deficient placentas

It is known that highly variable patterns of DMD methylation and imprinted-gene expression observed among DNMT1o-deficient embryos are accompanied by a highly variable embryonic morphology (Toppings et al. 2008). This relationship suggests that deviation from strict parent-specific DMD methylation and monoallelic expression leads to defects in embryonic development. Given DNMT1o-deficient placentas also had significant variability in DMD methylation at E9.5, we sought to determine if DNMT1odeficient placentas were structurally abnormal early in gestation. Using cell- and tissuespecific markers we identified multiple structural anomalies in a DNMT1o-deficient placentas compared to an E9.5 wt control (39 DNMT1o-deficient placentas analyzed). A representative litter is shown in Figure 4. For example, an expanded giant cell layer (*Prl2c2* probe) was observed in three out of seven mutant placentas (M4, M5 and M10). Moreover, structural distortions of the spongiotrophoblast layer (*Tpbpa*) and labyrinth (*Tfeb*) were common (M5, M6, M7 and M8). Only two Dnmt1o-deficient placentas, M9 and M10, had normal morphology.

To describe the spatial expression pattern of imprinted genes in Dnmt1o-deficient placentas we probed the same placentas for expression of *Ascl2, Phlda2* and *Igf2* (Figure 4). The imprinted gene *Ascl2*, normally expressed in both the labyrinth and spongiotrophoblast, displayed variable expression in DNMT1o-deficient placentas, ranging from patchy, mosaic expression in the labyrinth and/or spongiotrophoblast (M6 and M7) to normal expression (M4, M9 and M10). *Phlda2* is expressed robustly in the wt labyrinth whereas the same mutants that had loss of *Ascl2* expression (M6 and M7) also had decreased *Phlda2* expression. The imprinted gene *Igf2* also displayed a great deal of variation in the mutants. In wt and two mutant (M9 and M10) placentas *Igf2* is ubiquitously expressed, with particularly high levels in the labyrinth. Five of the mutants (M4–M8) had severely restricted *Igf2* expression as compared to wt. This data supports the notion that Dnmt1o-deficient placentas are mosaic for the expression of imprinted genes.

Our DMD methylation and imprinted gene expression data from E17.5 differed from our findings at E9.5. Given this we sought to determine the impact of DNMT1o deficiency on fetal viability, fetal growth, and placental morphology in late gestation (E17.5). Table 1 demonstrates the percentage of embryos that were alive at E9.5, E12.5, E15.5, and E17.5. At E17.5, 34/59 (from 9 litters) DNMT1o-deficient fetuses were alive versus 20/20 (3 litters) wt fetuses. Despite the decline in fetal viability across gestation, the relatively large number of fetuses recovered at E17.5 indicates that a proportion of E9.5 mosaic placentas are capable of further growth and development. Interestingly, as seen in Figure 5F and 5G, E17.5 DNMT1o-deficient embryos and placentas were larger than wt. When embryo to placental (E/P) weight, an indicator of placental efficiency, was plotted, wt embryos clustered tightly around a mean E/P ratio of 10.0 (Figure 5F). Among DNMT1o-deficient conceptuses, there was significant variation in the E/P ratio, with a mean E/P ratio of 8.2. The fetal gender was not significantly related to E/P ratio in either wt or DNMT1o-deficient conceptuses. Interestingly, in the DNMT1o-deficient placentas only *Ascl2* and *Mest* expression were significantly ($p < 0.01$ for both) related to the E/P ratio—*Ascl2* in an inverse fashion and *Mest* in a direct fashion (Supplemental Figure 1). In multivariable linear regression modeling the expression of *Ascl2* and *Mest* accounted for 82% of the variance in E/P ratio among DNMT1o-deficient conceptuses. This relationship remained significant when controlling for gender ($p < 0.001$).

To gain insight into the consequence of disrupted imprinting on placental morphology late in gestation we again used standard histological, ISH, and immunohistochemical methods to examine a large series of E17.5 placentas. As shown in Figure 5A, H&E stained sections of wt E17.5 placentas revealed organized placentas with clearly identifiable layers. In contrast, the histomorphology of representative DNMT1o-deficient E17.5 placentas was widely variable. No DNMT1o-deficient placentas with wild type morphology were seen. Interestingly, fetuses within the high E/P category possessed better organized placentas, whereas those within the low E/P category had placentas with a disorganized structure. The dominant DNMT1o-deficient phenotype—seen in approximately 60% of placentas with viable embryos—was characterized by a slightly enlarged spongiotrophoblast layer with small invaginations of spongiotrophoblast into the labyrinth (Figure 5B–E). Quantification of the volume fraction of spongiotrophoblast and labyrinth in wt and DNMT1o-deficient (low and high E/P ratios combined) placentas revealed an increased median volume fraction of spongiotrophoblast and decreased labyrinth volume in DNMT1o-deficient placentas compared to wt. The marked variation of volume fractions of the layers in DNMT1odeficient placentas compared to wt was also evident (Figure 5I–J). Expression of lineage specific marker genes was not different by E/P ratio (data not shown). Given the modest differences in overall volume fraction of the layers this is not surprising. Placentas with low E/P ratios (smaller embryos) had more extensive projections of spongiotrophoblast into the labyrinth (Figure 5D and 5E) with a greater disorganization between the layers. Finally, while a thickened giant cell layer was seen in some DNMT1o- deficient placentas, a consistent abnormality of the giant cell layer was not observed (data not shown).

We then used ISH for *Tpbpa* expression and PAS staining to better define the defects in the spongiotrophoblast layer of DNMT1o-deficient placentas. The expression pattern of *Tpbpa* confirmed the ectopic location of spongiotrophoblasts in the labyrinth of DNMT1o-deficient placentas (Figure 6A–6D). On H&E staining, the spongiotrophoblast layer of DNMT1o-deficienct placentas contained more intracytoplasmic vacuoles compared to wt. These were PAS positive, suggesting that many of these spongiotrophoblasts were glycogen cells (Figure 6F and G). Interestingly, placentas with lower E/P ratios (smaller embryos) had less intracytoplasmic vacuoles and less PAS positive cells in spongiotrophoblast layer than placentas with larger embryos (Figure 6H vs. 6F and 6G and Figure 5B and 5C vs. 5D and 5E).

We used CD31 immunostaining and ISH to the leptin receptor to further examine the structure of the labyrinth. While the labyrinth of DNMT1o-deficient placentas is larger than the labyrinth of wt placentas, the combined surface area of fetal endothelium and maternal blood pools is less in mutant placentas −512 +/− 98 cm^2/cm^3, than wt-−790 +/− 100 cm^2/cm^3 ($p < 0.01$). This lack of fetal vasculature development was evident in all placentas (Figure 7) but was more notable in conceptuses with a low E/P ratio (Figure 7I and J) compared to those with a high E/P ratio (Figure 7G and H).

Notably, despite the disruption of the normal architecture of the late-gestation placentas, the observed histomorphological abnormalities were uniform across sections. We sought to determine if the loss of DNA methylation at imprinted domains in E17.5 placentas was also uniform. To assess this we quartered E17.5 DNMT1o-deficient placentas and characterized DNA methylation at 5 imprinted gene clusters—*H19/Igf2, Kcnq1, Mest, Igf2r, and Gtl2*- in separate quarters using the EpiTYPER application. This demonstrated a high degree of correlation in methylation between quarters of individual placentas at all five imprinted loci (Supplementary Figure 2).

Deficiency of DNMT1o induces transcriptional changes

We used gene expression microarrays to identify differences in gene expression between DNMT1o-deficient placentas with high and low E/P ratios (n=4 for each group). The dendrogram in Figure 8A shows that each group clustered together and that high E/P placentas were more similar in patterns of gene expression to wt placentas than the low E/P placentas. To identify biologically meaningful genes between placental phenotypes, only genes with a false discovery rate (FDR/ q-value) < 0.05 were considered significant. Data were then analyzed with Ingenuity Pathway Analysis (IPA). As seen in Figure 8B, there was significant overlap between both placental phenotypes among down-regulated genes, with at least 75% of the genes down-regulated 1.3 fold in high E/P ratio placentas also down-regulated in low E/P ratio placentas. Functional analysis with IPA identified genes involved in the oxidative stress response as commonly down-regulated genes. Less overlap was seen among genes that were up regulated in both phenotypes. Among genes that were up-regulated in both high and low E/P ratio placentas, IPA identified genes involved in lipid metabolism, specifically genes regulating the accumulation of lipids. Among genes that were up regulated only in placentas with high E/P ratio both transport of small molecules and lipids. (Figure 8C). Importantly, these transcriptional findings likely reflect both the loss of imprinting in DNMT1o-deficient placentas as well as the change in cellular demographics due to altered placental structure in DNTM1o mutants.

DISCUSSION

Stochastic elimination of DMD methylation at many sites during preimplantation development has a profound impact on placental development and fetal growth that evolves across gestation. At E9.5 the majority of embryos are alive and a broad range of placental abnormalities are seen. By E17.5 there is a decline in fetal viability and among surviving embryos a broad range of fetal weights and E/P ratios are seen. Furthermore, while placental morphology is always abnormal at E17.5, the range of abnormalities is narrower than that seen at E9.5. These changes in placental morphology and fetal weight parallel significant changes in DMD methylation and expression in imprinted genes. At E9.5 loss of DMD methylation is seen at all DMDs we examined. In contrast, at E17.5 among the placentas we examined, statistically significant loss of methylation is not seen at either the *H19* or *Kcnq1* DMDs. The expression of imprinted genes also changes across gestation. At E9.5 imprinted gene expression largely mirrors the expression one would predict based on loss of DMD methylation. At E15.5 and E17.5, however, we observe imprinted gene expression that is contrary to expectations based on loss of methylation. We speculate that these findings reflect changes in the cellular demographics of the placenta or significant attrition and/or acceleration of growth of certain cells with particular DMD methylation patterns—or epigenotypes. The range of morphologic abnormalities we see at E9.5 compared to E17.5 may also reflect a greater diversity of epigenotypes at E9.5. Finally, the changes in profiles of imprinted-gene expression across the later half of gestation, particularly the changes between E12.5 and E15.5, suggests that expression of imprinted genes is governed by factors other than the methylation of its controlling DMD.

The kinship or parental conflict hypothesis is the most widely accepted hypothesis to explain the evolution of imprinted genes (Moore and Haig 1991). It argues that imprinted genes evolved to balance maternal and paternal contributions to fetal growth. Consistent with the parental conflict hypothesis, the majority of paternally expressed genes promote fetal growth maximizing the reproductive fitness of offspring. In contrast, maternally expressed genes tend to restrict fetal growth allowing for offspring survival, but minimizing the resource drain to the mother who will reproduce again in the future. Given this general model, a widespread disruption of imprints during preimplantation development would be predicted to widen the distribution of fetal weights. Our findings are consistent with this (Figure 5F).

Embryos that develop in the absence of DNMT1o display a broad range of fetal weights suggesting that important checks on establishing a normal range of fetal growth have been disturbed. Dissecting the mechanisms underlying the different sizes of these fetuses will improve our understanding of determinants of fetal growth- both fetal growth restriction as well as fetal macrosomia.

How might defects in placental imprinting in DNMT1o-deficient placentas contribute to fetal weight? In the case of small embryos (low E/P ratio), the poor fetal growth likely reflects both abnormal placental development as well as abnormal placental function. DNMT1o-deficient placentas have a reduced labyrinth zone and poor fetal vasculature development. This likely reduces the functional surface area available for maternal-fetal exchange of gases and nutrients. Additionally, most DNMT1o-deficient placentas have spongiotrophoblast tissue within the labyrinth layer. This may reflect a migration defect of the spongiotrophoblasts during development or a primary labyrinthine defect that led the spongiotrophoblast to proliferate in an ectopic location. Regardless, this contributes to the reduction in size of the labyrinth layer seen in these placentas. The finding of glycogen cells in the ectopic spongiotrophoblast tissue may have further implications for fetal growth. Glycogen cells migrate to the maternal decidua late in gestation and are thought to be a potential source of easily available glucose for the fetus late in gestation (Coan et al. 2006). Thus the mislocalization of glycogen cells in the labyrinth may limit extraembyronic energy stores late in gestation and impact fetal growth.

The glycogen cell phenotype seen in DNMT1o-deficient placentas is similar to that seen when *Phlda2* is overexpressed (Tunster et al., 2010). In this investigation, fetal growth restriction developed late in gestation and the junctional zone was reduced. In contrast, in DNMT1o-deficient placentas the junctional zone is expanded. This finding may be particularly critical because despite disorganized placentas, many of the DNMT1o-deficient placentas supported normal to supranormal fetal growth. Given the increased size of the junctional zone this suggests this layer may be particularly critical for regulating fetal growth in the DNMT1o model. The junctional zone is largely responsible for the endocrine function of the placenta and the size of junctional zone has been related to fetal weight in some mouse strains (Tunster et al., 2012). Additionally, our microarray analysis comparing DNMT1o-deficient placentas with low and high E/P ratios suggests that lipid metabolism and transport is particularly important in the altered E/P ratio conceptuses.

The findings from DNMT1o-deficient placentas, including placentomegaly, invaginations of spongiotrophoblasts into the labyrinth, and abnormal fetal vasculature, are similar to the placental phenotype from mouse interspecific hybrids (Zechner et al. 1996, Zechner et al. 1997, Zechner et al 2004, Duselis, Vrana 2010). A number of postzygotic mechanisms lead to reproductive isolation in interspecific hybridization, including placental dysplasia. Furthermore, disruption of genomic imprinting contributes to the placental dysplasia in interspecific hybridizaiton (Zechner et al. 2004, Shi et al. 2005). Given the similarity in placental phenotypes between DNMT1o-deficient placentas and those from interspecific hybrids it is possible that altered function of DNMT1o contributes to post-zygotic reproductive isolation in interspecific crosses.

Overall, our findings of wide-ranging E/P ratios in DNMT1o-deficient conceptuses also support the idea that a subset of imprinted genes is vitally important in placental function. Placental expression of genes from two imprinted clusters—*Ascl2* and *Mest*— accounts for a significant proportion of the observed variation in E/P ratio among DNMT1o-deficient placentas. There was a direct correlation between *Mest* expression and E/P ratio, and an inverse correlation between *Ascl2* and E/P ratio. Our methylation studies late in gestation indicate that loss of methylation at the Peg1 DMD is tolerated late in gestation. Furthermore,

Mest expression is predicted to increase with loss of DMD methylation. In mouse placentas, *Mest* expression is limited to tissues derived from extraembryonic mesoderm, in late gestation it is localized to capillary endothelial cells of the placental labyrinth. Investigations suggest that *Mest* is involved in angiogenic sprouting in labyrinth (Mayer et al., 2000). While a targeted mutation of *Mest* was associated with growth retardation and a reduction in the size of the placenta, the placental phenotype was not described in detail (Lefebvre et al., 1998). Given that as whole DNMT1o-deficient placentas have a reduced volume fraction of the labyrinth, increased *Mest* expression may be an important compensatory response in DNMT1o placentas. Our data support the importance of further investigation to determine the precise function of imprinted genes in the *Mest* cluster.

Another important consideration in our findings is the interaction between the fetus and the placenta in determining the nutrients available to sustain fetal growth. The placenta responds to fetal signals for increased nutrient demand. While the fetal signals that influence placental growth and development are not well characterized, imprinted genes expressed in the fetus have been shown to play a role (Constancia et al., 2005). Nevertheless, the combination of fetal and placental DMD mosaicism in the $Dnmt1^{\Delta 1o}$ model allows us to examine critical relationships among placental DMD methylation, placental development, and fetal growth.

Supplementary Material

Refer to Web version on PubMed Central for supplementary material.

Acknowledgments

We thank Dr. Jacquetta Trasler for assistance with preliminary studies of the DNMT1o-deficient placentas, Dr. Serge McGraw for technical advice with EpiTyper studies, Dr. Tianjiao Chu for assistance with statistical analysis of arrays, Drs. Yaacov Barak and Yoel Sadovsky for both technical guidance and critical reading of the manuscript, and Ben Shaffer and Ashwini Balakrishnan for technical assistance. This work is supported by NIH Grant R01 HD044133 (to J.R.C.) and the Reproductive Scientist Development Program grant NIH K12 HD000849 (to K.P.H.).

REFERENCES

Baddeley AJ, Gundersen HJ, Cruz-Orive LM. Estimation of surface area from vertical sections. J. Microsc. 1986; 142:259–276. [PubMed: 3735415]

Barak Y, Nelson MC, Ong ES, Jones YZ, Ruiz-Lozano P, Chien KR, Koder A, Evans RM. PPAR gamma is required for placental, cardiac, and adipose tissue development. Mol. Cell. 1999; 4:585–595. [PubMed: 10549290]

Bartolomei MS, Tilghman SM. Genomic imprinting in mammals. Annu. Rev. Genet. 1997; 31:493–525. [PubMed: 9442905]

Bourc'his D, Xu GL, Lin CS, Bollman B, Bestor TH. Dnmt3L and the establishment of maternal genomic imprints. Science. 2001; 294:2536–2539. [PubMed: 11719692]

Cirio MC, Ratnam S, Ding F, Reinhart B, Navara C, Chaillet JR. Preimplantation expression of the somatic form of Dnmt1 suggests a role in the inheritance of genomic imprints. BMC Dev. Biol. 2008a; 8:9. [PubMed: 18221528]

Cirio MC, Martel J, Mann M, Toppings M, Bartolomei M, Trasler J, Chaillet JR. DNA methyltransferase 1o functions during preimplantation development to preclude a profound level of epigenetic variation. Dev. Bio. 2008b; 324:139–150. [PubMed: 18845137]

Coan PM, Ferguson-Smith AC, Burton GJ. Developmental dynamics of the definitive mouse placenta assessed by stereology. Biol. Reprod. 2004; 70:1806–1813. [PubMed: 14973263]

Coan PM, Conroy N, Burton G, Ferguson-Smith AC. Origin and characteristic of glycogen cells in the developing murine placenta. Dev. Dyn. 2006; 235:3280–3294. [PubMed: 17039549]

Constancia M, Angiolini E, Sandovici I, Smith P, Smith R, Kelsey G, Dean W, Ferguson-Smith AC, Sibley CP, Reik W, Fowden A. Adaptation of nutrient supply to fetal demand in the mouse involves

interaction between the *Igf2* gene and placental transporter systems. Proc. Natl. Acad. Sci. 2005; 102:19219–19224. [PubMed: 16365304]

Doherty AS, Bartolomei MS, Schultz RM. Regulation of stage-specific nuclear translocation of Dnmt1o during preimplantation mouse development. Dev. Biol. 2002; 242:255–266. [PubMed: 11820819]

Duselis AR, Vrana PB. Aberrant growth and pattern formation in Peromyscus hybrid placental development. Biol. Reprod. 2010; 83:988–996. [PubMed: 20702850]

Ehrich M, Nelson MR, Stanssens P, Zabeau M, Liloglou T, Xinarianos G, Cantor CR, Field JK, van den Boom D. Quantitative high-throughput analysis of DNA methylation patterns by base-specific cleavage and mass spectrometry. Proc. Natl. Acad. Sci. 2005; 102:15785–15790. [PubMed: 16243968]

Frost JM, Moore GE. The importance of imprinting in the human placenta. PLoS Genetics. 2010; 6 e1001015.

Guillemot F, Nagy A, Auerback A, Rossant J, Joyner AL. Essential role of Mash-2 in extraembryonic development. Nature. 1994; 22:333–336. [PubMed: 8090202]

Hata K, Okano M, Lei H, Li E. Dnmt3L cooperates with the Dnmt3 family of de novo DNA methyltransferases to establish maternal imprints in mice. Development. 2002; 129:1983–1993. [PubMed: 11934864]

Hirasawa R, Chiba H, Kaneda M, Tajima S, Li E, Jaenisch R, Sasaki H. Maternal and zygotic Dnmt1 are necessary and sufficient for the maintenance of DNA methylation imprints during preimplantation development. Genes Dev. 2008; 22:1607–1616. [PubMed: 18559477]

Howell CY, Bestor TH, Ding F, Latham KE, Mertineit C, Trasler JM, Chaillet JR. Genomic imprinting disrupted by a maternal effect mutation in the Dnmt1 gene. Cell. 2001; 104:829–838. [PubMed: 11290321]

Kaneda M, Okano M, Hata K, Sado T, Tsujimoto N, Li E, Sasaki H. Essential role for de novo DNA methyltransferase Dnmt3a in paternal and maternal imprinting. Nature. 2004; 429:900–903. [PubMed: 15215868]

Lefebvre L, Viville S, Barton SC, Ishino F, Keverne EB, Surani MA. Abnormal maternal behaviour and growth retardation associated with loss of the imprinted gene Mest. Nat. Genet. 1998; 2:163–169. [PubMed: 9771709]

Lucifero D, Mertineit C, Clarke HJ, Bestor TH, Trasler JM. Methylation dynamics of imprinted genes in mouse germ cells. Genomics. 2002; 79:530–538. [PubMed: 11944985]

Mayer W, Hemberger M, Frank HG, Grummer R, Winterhager E, Kaufmann P, Fundele R. Expression of the imprinted genes MEST/Mest in human and murine placenta suggests a role in angiogenesis. Dev. Dyn. 2000; 217:1–10. [PubMed: 10679925]

Moore T, Haig D. Genomic imprinting in mammalian development: a parental tug of war. Trends Genet. 1991; 2:45–49. [PubMed: 2035190]

Ono R, Nakamura K, Inoue K, Naruse M, Usami T, Wakisaka-Saito N, Hino T, Suzuki-Migishima R, Ogonuki N, Miki H, Kohda T, Ogura A, Yokoyama M, Kaneko-Ishino T, Ishino F. Deletion of Peg10, an imprinted gene acquired from a retrotransposon, causes early embryonic lethality. Nat. Genet. 2006; 38:101–106. [PubMed: 16341224]

Reinhart B, Eljanne M, Chaillet JR. Shared role for differentially methylated domains of imprinted genes. Mol. Cell Biol. 2002; 22:2089–2098. [PubMed: 11884597]

Reinhart B, Chaillet JR. Genomic imprinting: cis-acting sequences and regional control. Int. Rev. Cytol. 2005; 243:173–213. [PubMed: 15797460]

Shi W, Drella A, Orth A, Yu Y, Fundele R. Widespread disruption of genomic imprinting in adult interspecies mouse (*Mus) hybrids. Genesis. 2005; 43:100–108. [PubMed: 16145677]

Toppings M, Castro C, Mills PH, Reinhart B, Schatten G, Ahrens ET, Chaillet JR, Trasler JM. Profound phenotypic variation among mice deficient in the maintenance of genomic imprints. Hum. Reprod. 2008; 23:807–818. [PubMed: 18276606]

Tunster SJ, Tycko B, John RM. The imprinted Phlda2 gene regulates extraembryonic energy stores. Mol. Cell Biol. 2010; 30:295–306. [PubMed: 19884348]

Tunster SJ, Van de Pette M, John RM. Impact of genetic background on placental glycogen storage in mice. Placenta. 2012; 33:124–127. [PubMed: 22153913]

Zechner U, Reule M, Orth A, Bonhomme F, Strack B, Guénet JL, Hameister H, Fundele R. An X-chromosome linked locus contributes to abnormal placental development in mouse interspecific hybrids. Nat. Genet. 1996; 12:398–403. [PubMed: 8630493]

Zechner U, Reule M, Burgoyne P, Schubert A, Orth A, Hameister H, Fundele R. Paternal transmission of X-linked placental dysplasia in mouse interspecific hybrids. Genetics. 1997; 146:1399–1405. [PubMed: 9258682]

Zechner U, Shi W, Hemberger M, Himmelbauer H, Otto S, Orth A, Kalscheuer V, Fischer U, Elango R, Reis A, Vogel W, Ropers H, Rüschendorg F, Funele R. Divergent genetic and epigenetic post-zygotic isolation mechanisms in Mus and Peromyscus. J. Evol. Biol. 2004; 17:453–460. [PubMed: 15009278]

HIGHLIGHTS

- Disruption of imprints alters the distribution of embryonic and placental weights
- Placentas have a disorganized morphology and an expanded spongiotrophoblast layer
- Nevertheless, fetal growth is often maintained or enhanced compared to wild type

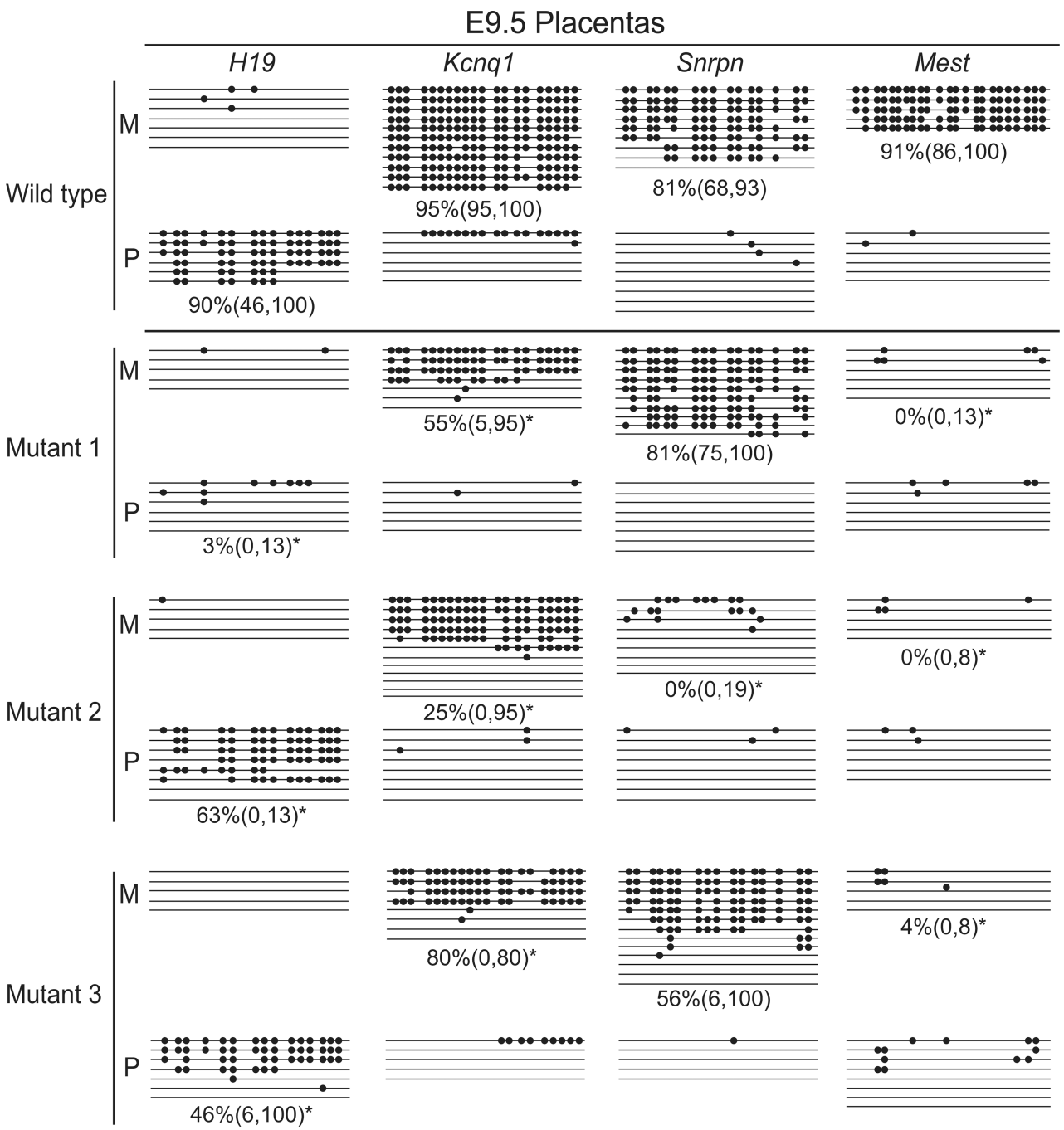

Fig. 1.

At E9.5, DNMT1o-deficient placentas have variable loss of DMD methylation at *H19, Kcnq1, Snrpn* and *Mest*. Methylation patterns of a representative wild type and three DNMT1o-deficient placentas are shown. M= maternal alleles. P= paternal alleles. Position of methylated CpGs dinucleotides are indicated as filled circles. The median methylation at the normally methylated allele is shown with the interquartile range in parentheses. * Denotes significantly different methylation of CpGs compared to wild type by Kruskal Wallis with $p<0.05$.

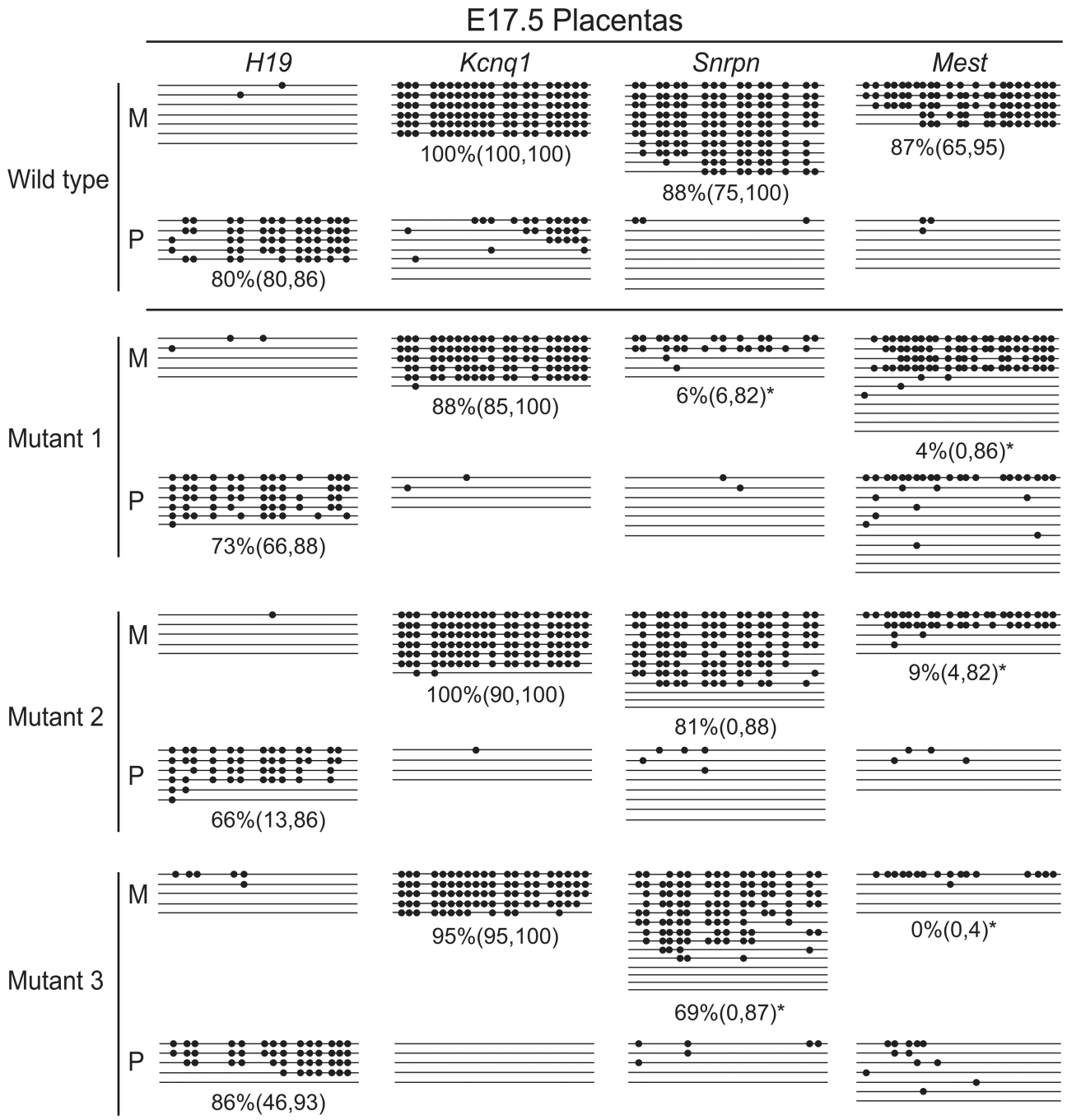

Fig. 2.

At E17.5, DNMT1o-deficient placentas have variable loss of DMD methylation at *Snrpn* and *Mest*, but DMD methylation at *H19* and *Kcnq1* did not differ from wild type in placentas examined. Methylation patterns of a representative wild type and three DNMT1o-deficient placentas are shown. M= maternal alleles. P= paternal alleles. Position of methylated CpGs dinucleotides are indicated as filled circles. The median methylation at the normally methylated allele is shown with the interquartile range in parentheses. * Denotes significantly different methylation of CpGs compared to wild type by Kruskal Wallis with $p<0.05$.

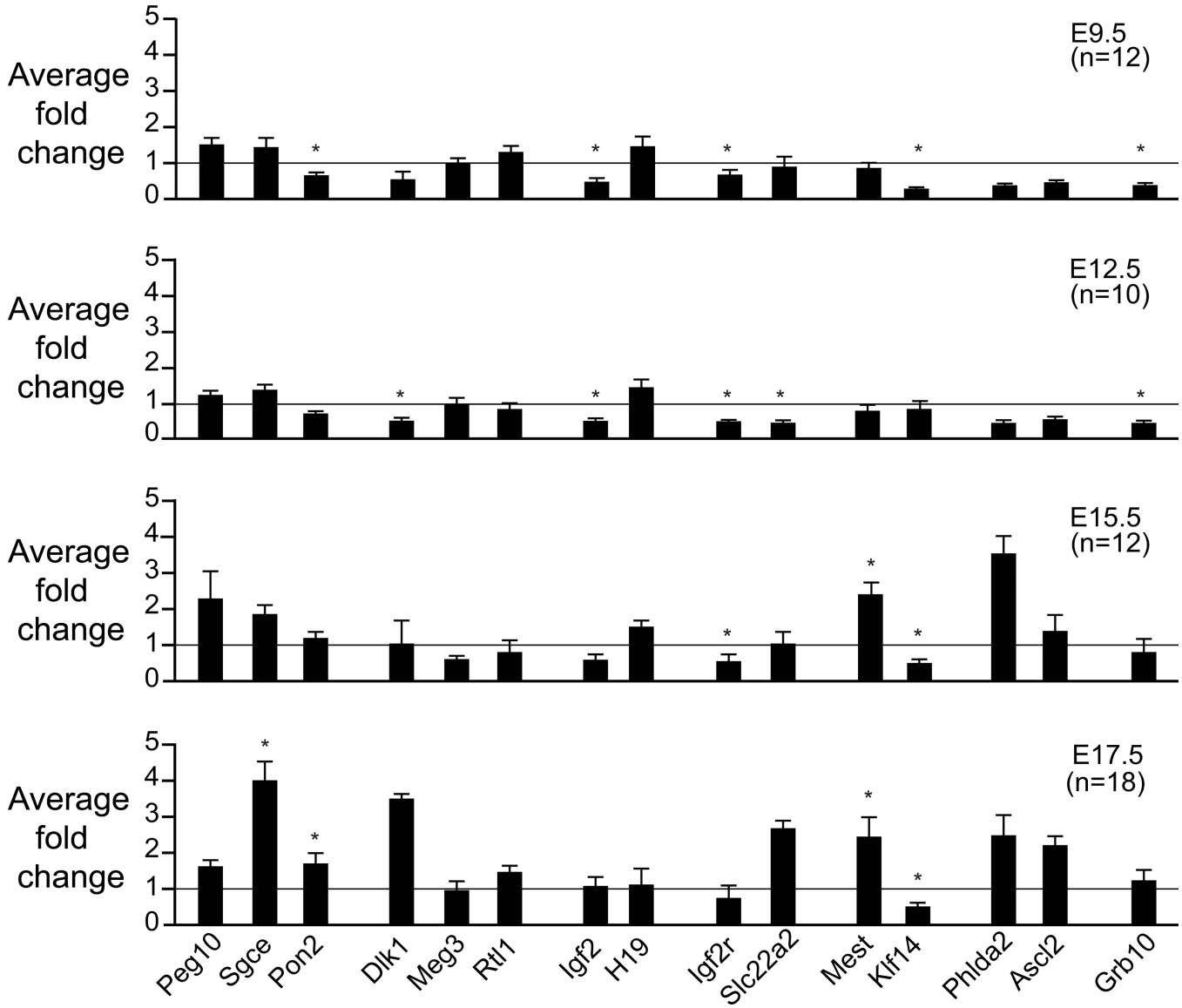

Fig. 3.

Expression of imprinted genes from DNMT1o-deficient placentas at E9.5, E12.5, E15.5 and E17.5 evolves across gestation. The histograms summarize mean expression (+SEM) of imprinted genes from seven imprinted gene clusters in DNMT1odeficient placentas compared to wild type (n=5). Each qPCR measurement was performed in triplicate, normalized to the L32 gene, and analyzed with the ΔΔCt method. (n=number of placentas studied). * Denotes significantly different expression compared to wild type by Kruskal Wallis with $p < 0.05$.

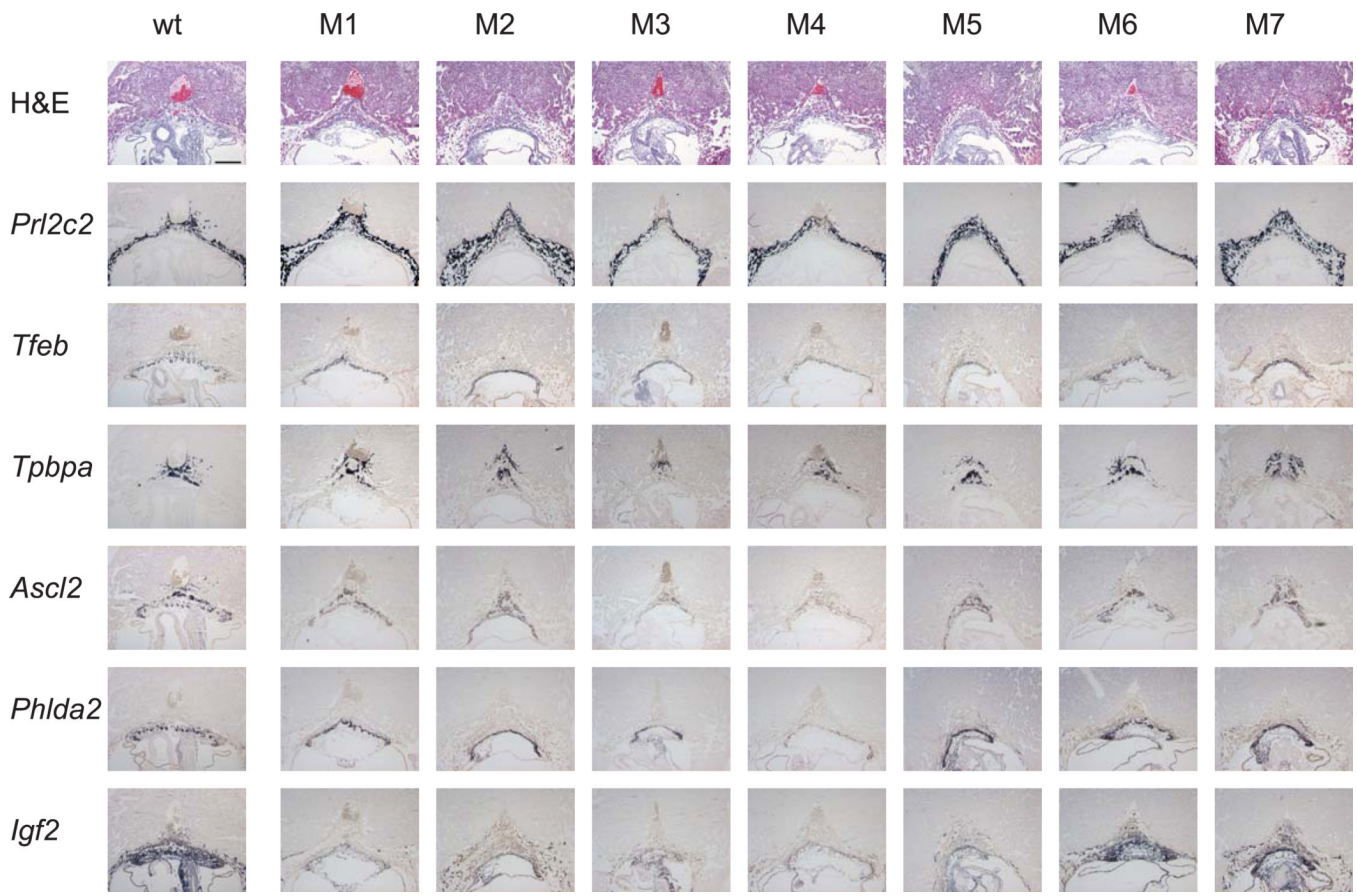

Fig. 4.

A broad range of morphologic and gene expression abnormalities is present in E9.5 DNMT1o-deficient placentas. Hematoxylin/Eosin (H&E) staining and in situ hybridization (ISH) of frozen sections of wt and DNMT1o-deficient E9.5 conceptuses from a single litter. Multiple sections from placentas of each genotype were assessed and representative sections are shown. Each column of sections was obtained from a single conceptus. ISH probes are listed on the left include placenta lineage markers *Prl2c2, Tpbpa* and *Tfeb* as well as the imprinted genes *Ascl2, Phlda2* and *Igf2*. wt= Wild type. M= DNMT1o-deficient mutant. Scale bar 500uM.

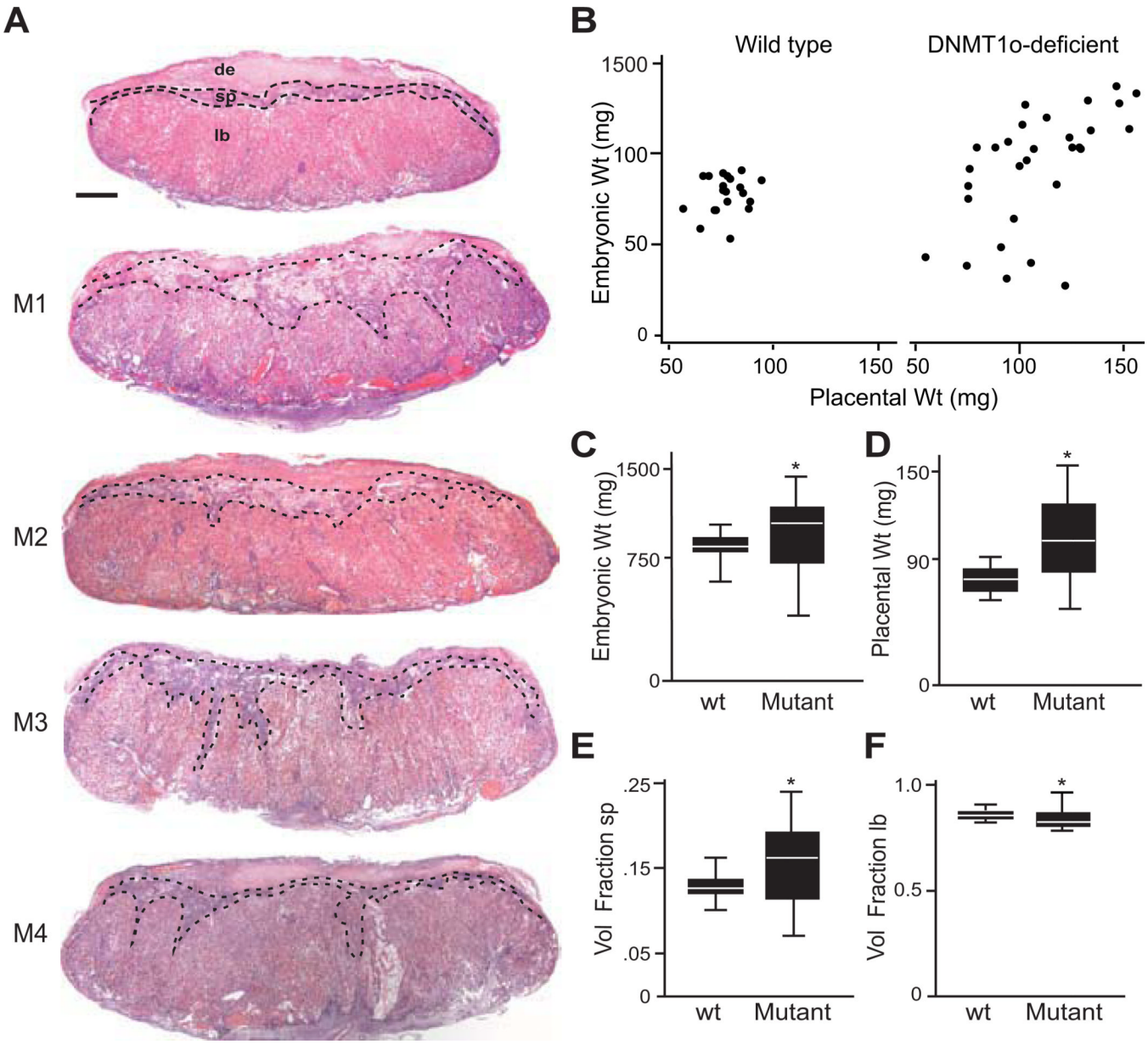

Fig. 5.

At E17.5, DNMT1o-deficient placentas demonstrate characteristic morphologic abnormalities and have a broader distribution of embryonic/placental (E/P) weight ratios compared to wild type. (A) H&E staining of paraffin-embedded placental sections at E17.5 with the labyrinth, spongiotrophoblast, and maternal decidua delineated. (B) Scatter plot of embryonic to placental weight of E17.5 wild type and DNMT1o-deficient conceptuses. (C, D) Box plots showing median values, upper and lower quartiles and range of embryonic and placental weights among wild type and DNMT1o-deficient conceptuses. (E,F) Stereologic analysis of volume fraction of spongiotrophoblast and labyrinth depicted as box plots. Scale bars, 400μm (A). wt= Wild type. M= DNMT1odeficient mutant. de= Decidua. sp= Spongiotrophoblast. lb= Labyrinth. *p <0.05 by Kruskal Wallis.

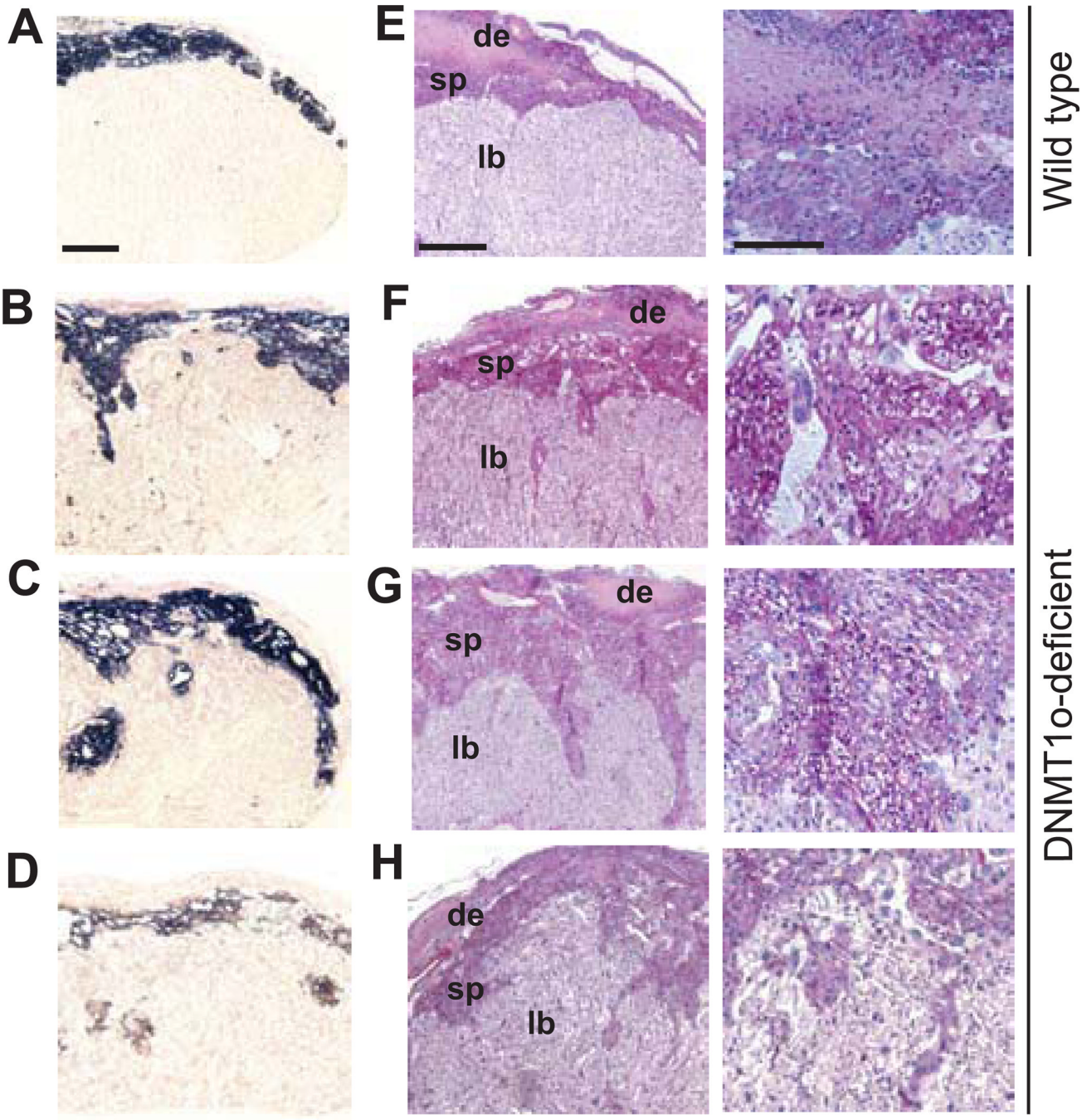

Fig. 6.

At E17.5, DNMT1o-deficient placentas had abnormal spongtotrophoblast layer and glycogen cell distribution. (A–D) ISH with *Tpbpa* in representative wild type and DNMT1o-deficient placentas. (E–H) PAS staining localizes glycogen staining largely to maternal decidua in wild type placentas. DNMT1o-deficient placentas have abnormal accumulation of glycogen in spongiotrophoblasts. This is prominent in most placentas examined (F,G) but less notable in other placentas (H). de= Decidua. sp= Spongiotrophoblast. lb= Labyrinth. Scale bar (A–D) 400μm, (E–H) 400μm (left panel) and 100μm (right panel).

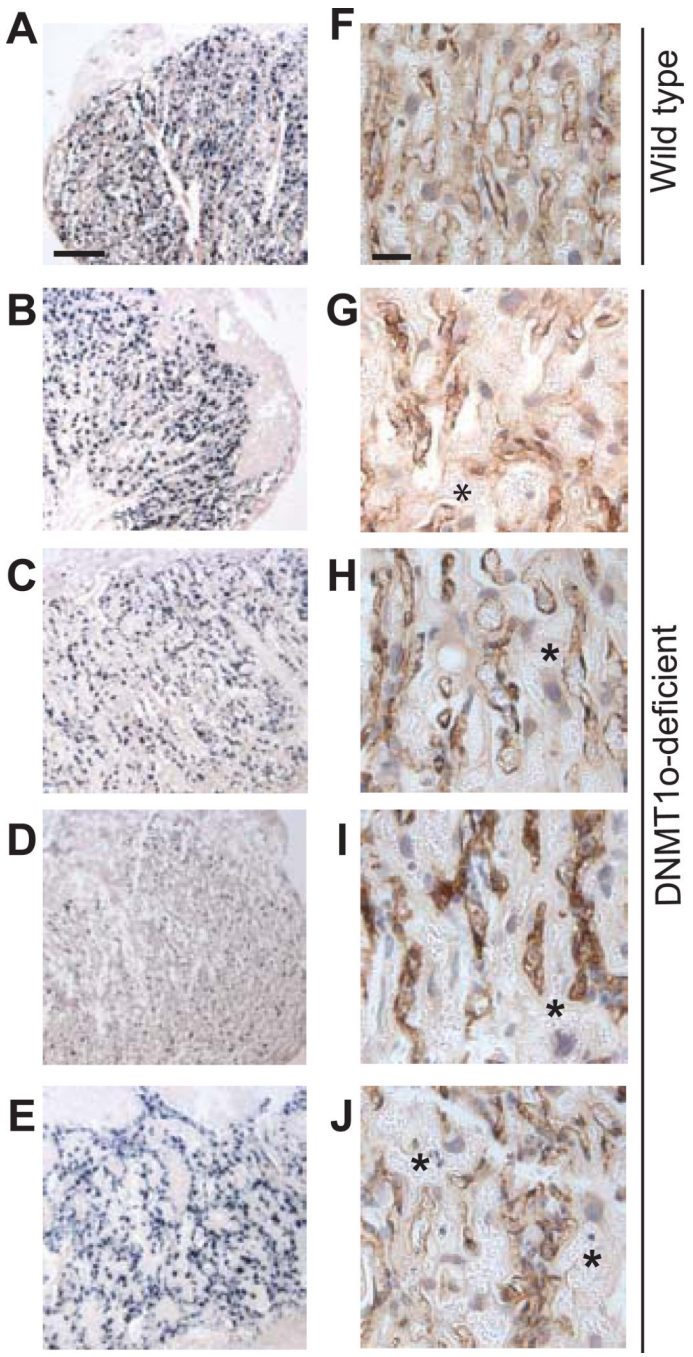

Fig. 7.

The labyrinth layer in DNMT1o-deficient placentas at E17.5 has both abnormal fetal vasculature and maternal blood pools. (A–E) ISH with Leptin receptor in representative wild type and DNMT1o-deficient placentas. Leptin receptor is present in the trophoblasts that line the maternal blood pools. (F–J) Immuno-staining with CD31 in wild type and DNMT1o-deficient placentas. * Maternal blood pools that are dilated in DNMT1o- deficient placentas. Scale bar (A–E) 400μm (F–J) 50um.

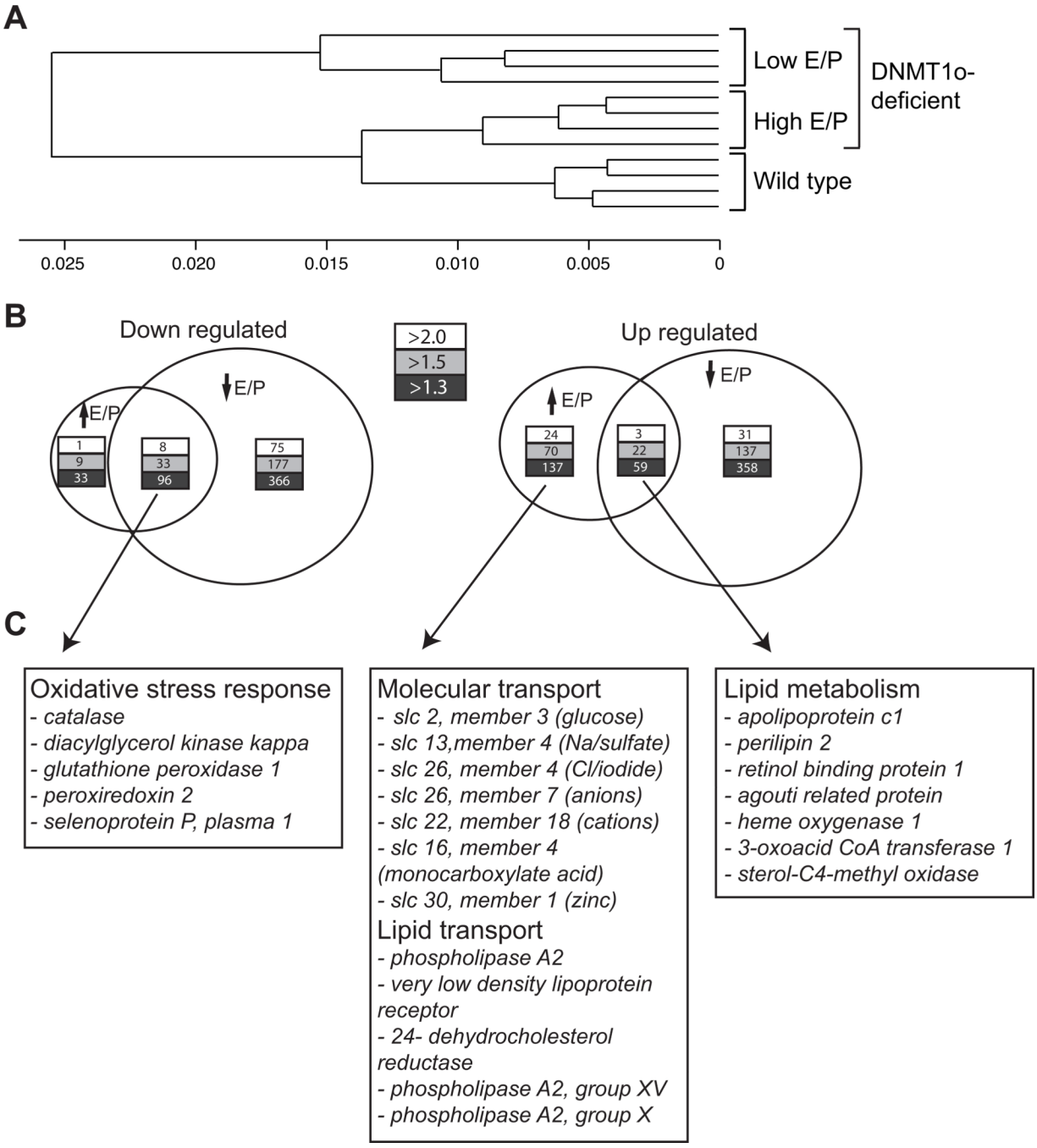

Fig. 8.

Shared and distinct gene expression patterns are present in E17.5 DNMT1odeficient placentas with distinct E/P ratios. (A) Dendrograms describing genome-wide expression differences in E17.5 placentas. The X-axis is 1 minus the correlation coefficient. The E17.5 DNMT1o-deficient placentas were pooled into two groups based on the ratio of embryo/placental weight ratio (E/P) ratio with 4 placentas in each group. (B) Venn diagrams show the proportion of over-lapping and distinct genes that are down or up regulated in placentas with either a high E/P ratio or a low E/P ratio. Genes were included for consideration at a q < 0.05. Data are stratified by fold changes, 2.0 (top), 1.5 (middle), and 1.3 (lower). (C) Gene

lists show results of functional analysis performed using Ingenuity Pathway Analysis. P value was less 0.01 for all genes in the functional analysis.

Table 1

Survival of embryos

Day of analysis	Number of litters		Number mutants viable per litter
	Wild type	Mutant	
E9.5	3	5	4.6
E12.5	3	5	3.1
E15.5	3	6	2.1
E17.5	3	7	2.5